

EFFECT OF ALIGNMENT ON THE QUALITY OF BENDER ELEMENT PROCEDURE

Badee Alshameri^{a*}, Ismail Bakar^b, Aziman Madun^c, Edy Tonnizam Mohamad^d

^aYemen Company for Investment in Oil and Minerals-YICOM, Sana'a, Yemen

^bRECESS, Faculty of Civil and Environmental Engineering Universiti Tun Hussein Onn Malaysia, 86400 Parit Raja, Batu Pahat, Johor, Malaysia

^cFaculty of Civil and Environmental Engineering, Universiti Tun Hussein Onn Malaysia, 86400 Parit Raja, Batu Pahat, Johor, Malaysia

^dGeoengineering and Geohazard Research Group, Department of Geotechnics and Transportaion, Faculty of Civil Engineering, Universiti Tekhologi Malaysia, 81310 UTM Johor Bahru, Johor, Malaysia

Article history

Received

6 July 2015

Received in revised form

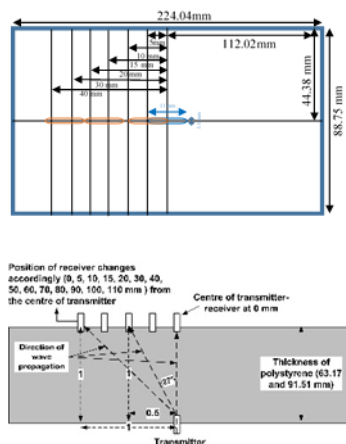
26 July 2015

Accepted

30 July 2015

*Corresponding author
badee.alshameri@yahoo.com

Graphical abstract



Abstract

One of the main geophysical tools (seismic tools) in the laboratory is the bender element. This tool can be used to measure some dynamic soil properties (e.g. shear and Young's modulus). However, even if it relatively simple to use the bender element, inconsistent testing procedures can cause poor quality in the bender element data. One of the bender element procedure that always neglected is the alignment (different positions of bender element receiver to the transmitter in the vertical axis). The alignment effect was evaluated via changing the horizontal distance between transmitter and receiver starting from 0 to 110 mm for two sizes of the sample's thickness (i.e. 63.17 mm and 91.51 mm). Five methods were applied to calculate the travel times. Those methods were as the following: visually, first-peak, maximum-peak, CC_{excel} and CC_{GDS} . In general, the experiments indicated uncertain results for both of the P-wave (primary wave) and S-wave (secondary wave) velocities at zone of $Dr:D$ above 0.5:1 (where Dr is the horizontal distance of the receiver from the vertical axis and D is the thickness of the sample). On the other hand, both the visual and first-peak methods show the wave velocities results are higher than obtained from other methods. However, the ratio between the amplitude of transmitter signals to receiver amplitude signal was taken to calculate the damping-slope of the P-wave and S-wave. Thus the results from damping slope show steeply slope when the ratio of $Dr:D$ is above 0.5:1 compare with gentle slope below ratio 0.5:1 at the sample with thickness equal to 91.51 mm, while there is no variation at a slope in sample with thickness equal to 63.17 mm.

Keywords: Bender element; procedure limitations; alignment; arrival time; cross-correlation

Abstrak

Salah satu alat geofizik dalam makmal yang berteraskan seismik adalah bender elemen. Alat ini digunakan untuk mengukur ciri-ciri dinamik tanah seperti modulus ricih dan modulus Young. mempunyai prosedur kerja yang mudah mengakibatkan prosedur ujian yang dijalankan tidak konsisten. Ini mengakibatkan data Bender elemen diperolehi berkualiti rendah. Salah satu prosedur bender elemen yang selalu diabaikan adalah penjajaran (kedudukan yang berbeza diantara unsur penerima dan pemancar dalam paksi menegak Bender elemen). Kesan penjajaran dinilai melalui perubahan jarak mengufuk antara pemancar dan penerima bermula dari 0 mm hingga 110 mm untuk dua saiz ketebalan sampel (iaitu 63.17 mm dan 91.51 mm). Lima kaedah telah digunakan untuk mengira masa perjalanan. Mereka kaedah adalah seperti berikut: visual, pertama-puncak, maksimum-puncak, CC_{excel} dan CC_{GDS} . Secara umum, keputusan ujian tidak menentu untuk kedua-dua kelajuan gelombang P (gelombang primer) dan S (gelombang kedua) apabila berada di zon Dr: D melebihi 0.5: 1 dan keatas (di mana Dr jarak mendarat penerima dari paksi menegak dan D adalah ketebalan sampel). Kaedah pengiraan menggunakan visual dan kaedah pertama-puncak menunjukkan kelajuan gelombang adalah lebih tinggi daripada dari kaedah lain. Seterusnya, nisbah antara amplitud isyarat pemancar dan penerima dianalisa untuk mengira cerun redaman gelombang P dan S. Hasilnya mendapati cerun redaman yang curam apabila nisbah Dr: D melebihi 0.5: 1 berbanding dengan cerun yang landai bagi nisbah kurang dari 0.5:1 bagi sampel dengan ketebalan 91.51 mm, manakala tidak ada perubahan pada cerun redaman pada sampel dengan ketebalan 63.17 mm

Kata kunci: Bender elemen; batasan prosedur; penjajaran; masa perjalanan; korelasi silang

© 2015 Penerbit UTM Press. All rights reserved

1.0 INTRODUCTION

The bender element is a useful geophysical tools to assess the physical properties of the soils such as shear and Young's modulus [1],[2],[3],[4],[5], [6],[7],[8],[9] Both of moduli can be calculated by a function of seismic wave velocity as:

$$E = V_p^2 \rho \quad (1)$$

$$G_0 = V_s^2 \rho \quad (2)$$

In which G_0 and E is the maximum shear and Young's modulus in the small strain range respectively. Meanwhile V_s and V_p is shear wave velocity and

compression waves velocity respectively, and ρ is bulk density.

The bender element is non-destructive test and appears deceptively simple. The input frequency use, the shear wave velocity of material and size of sample is controlled the testing procedure. These parameters can influence the arrangement of the transmitter and receiver. Therefore, the use of bender element to determine the shear wave velocity in repeatable has remained a challenge [10]. As a result, the testing procedure needs to establish. The bender element consists of the natural of electro-pressure properties of the piezoceramic, which can function to generate and receive the waves via vibrating, and thus converted this movement to electrical current with specific voltage and vice versa [1], [8], [11], [12].

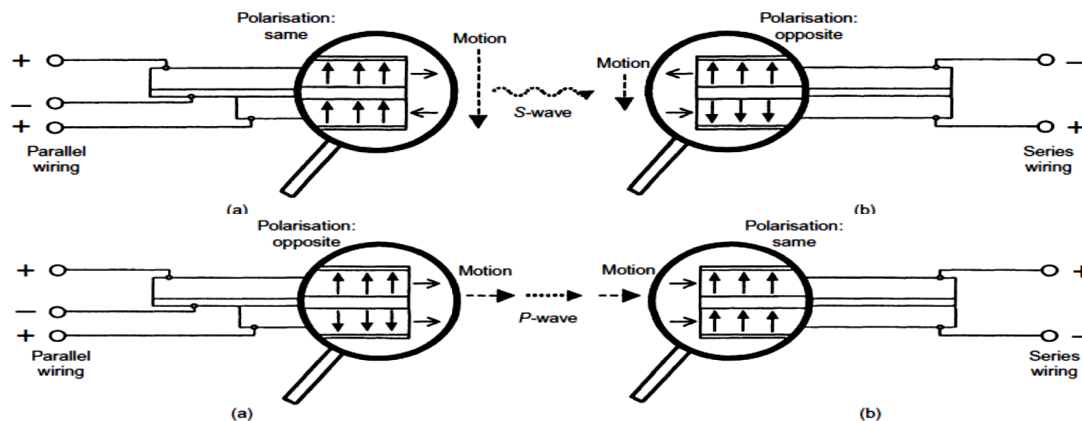


Figure 1 Polarisation and displacement details in extender bender element (a) transmitter; (b) receiver [13]

Moreover, Lings and Greening [13] gave details about the components of the extender bender element, which is the development of bender element (Figure 1).

According to Leong *et al.* [1], the way of working for extender bender element can be controlled by the configurations and polarization of the bender element (BE) sensors. Figure 1 shows both types of polarization (x-poled and y-poled) with series and parallel wiring configuration. However, using both of wiring configuration give ability to send and receive compression wave (P-wave) and shear wave (S-wave) directly without changing in the wiring [1], [13]. The aim of the study described in this paper is to understand the effect of the position of the alignment between the transducer and receiver in order to improve the objectivity and repeatability of the bender element shear wave velocity measurement.

well as repeated tests. Therefore, the soil samples were replaced by the polystyrene as shown in Figure 2 [1], [2]. The polystyrene is prepared to allow movement the top sensor in horizontal distance (D_r) away from the below sensor. Thus, the horizontal distance (D_r) versus the vertical axis (i.e. thickness of the sample D) is changed. The top BE sensor was put in position starting from 0 mm distance (where $D_r:D$ equal to 0:1). Then it was moved to 5, 10, 15, 20, 30, 40, 50, 60, 70, 80, 90, 100 and 110 mm horizontal distance from the vertical axis of bottom BE as shown in Figure 3. Two sizes of the samples were used in this research, (1) 63.17 mm x 224.75 mm x 88.75 mm, height, length and width, and density of 2.52×10^{-4} kN/m³ and (2) 91.51 mm x 224.81 mm x 62.45 mm height, length and width

2.0 METHODOLOGY AND PRINCIPLES

In this research, pair of sensor of extender bender element (BE) was used. Three limitations were faced in this research: (1) Short length of sensor intruded (about 1 mm) which caused poor contact between the BE sensor and compacted soil sample; (2) preparing suitable size of soil sample with fit dimension without disturbing the soil sample. (3) Maintain the moisture content of the soil samples due to the relative long period which taken to implement a series of test as

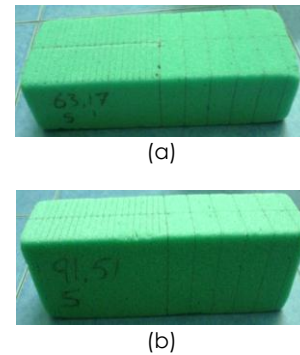


Figure 2 Polystyrene samples (a) thickness equal to 63.17 mm; (b) thickness equal to 91.51 mm

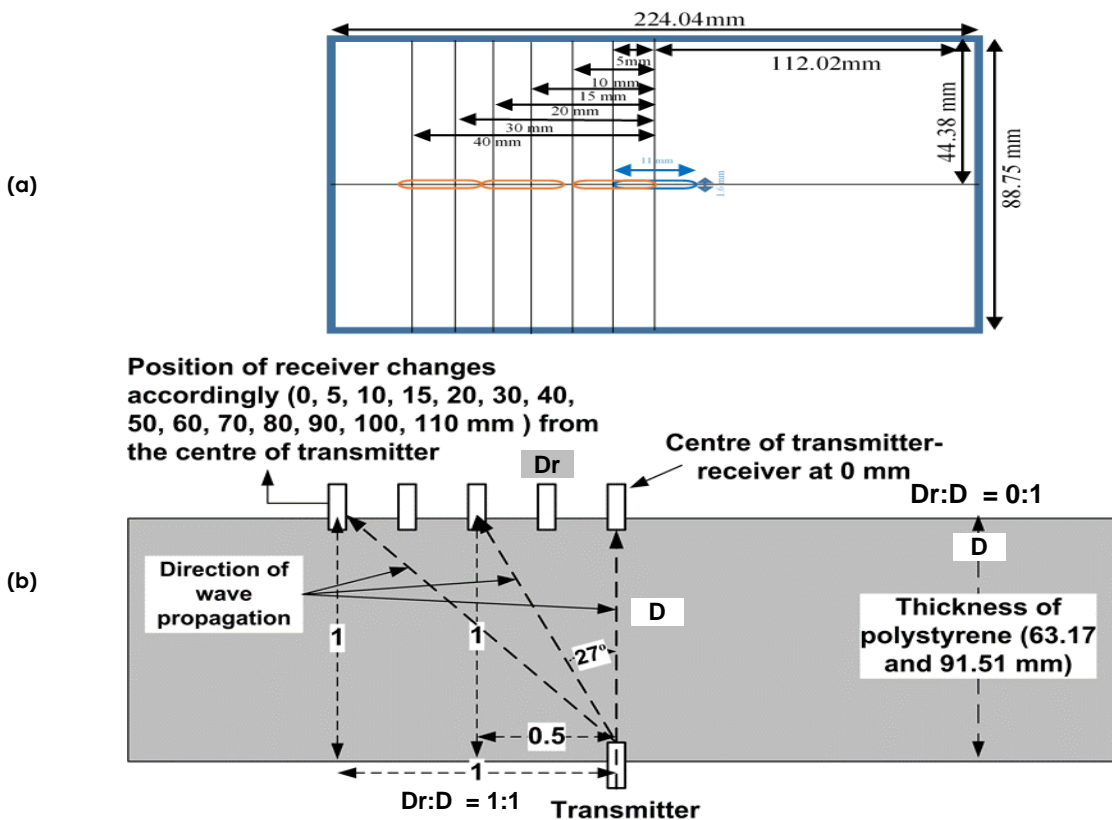


Figure 3 Position for the top cap of BE (the dimensions in the sketch are relative) (a) Top view (b) Side view

and density $2.51 \times 10^4 \text{ kN/m}^3$ (Figure 2). Many researchers such as: Leong *et al.* [1], Jovicic *et al.* [6], Leong *et al.* [14], Alamahi [15], Sa'nchez-Salinero *et al.* [16], Knox *et al.* [17] recommended to use the ratio of wave path length to wavelength above 4 to avoid the near field effect. Thus, in this research the 30 kHz frequency seismic source able to avoid this problem.

The tip to tip (tip of transmitter to tip of receiver) was considered as the distance to use in the wave velocities calculations [8], [18], [19] according to the following equation:

$$V = \frac{L_{tt}}{t} \quad (3)$$

In which V is the wave velocity for either P-wave or S-wave, L_{tt} is the wave path length from transmitter tip to the receiver tip and t is the recorded time.

2.1 Methods to Calculate Wave Arrival Time and Damping-Slope

Five methods were used to analyse the results and provide the P-wave and S-wave velocities. Visually, first-peak, maximum-peak, cross-correlation (CC_{excel}) by using excel and cross-correlation (CC_{GDS}) from GDS bender element analysis tools (GDS is Geotechnical Digital Systems Company for supplying geotechnical instruments).

First method, was visual record, it was taken directly from the software of GDS bender element version 1.5.3, which detected visually from the screen of the software and recorded with the original data that resulted from the software. The second method, was first-peak, it was calculated from the data and normalized data (normalized source and receiver) [1], [8], [14], [18], [19], [20]. The normalized data were calculated according to the maximum positive value. The third method was the maximum – peak where the arrival time is calculated according to the maximum peak of receiver compare with peak of the transmitter. It was calculated from both of data and normalized data. However, in fourth and fifth methods the cross-correlation method was used. In general, the cross-correlation methods are one of effective methods for analysis two wave signals in time domain by correlated both of them and provide the corresponding time for the best similarity between the two signals [14], [19], [20].

Fourth method was using cross-correlation by using excel software. This method was called CC_{excel} . Moreover, even there are different correlation point were used in CC_{excel} (cross-correlation from excel) (i.e. 4, 5, 6, 9, 15, 18, 27 and 52 correlative points) only the 4, 5 and 6 points are used in this research. The reason to use this point was the used frequency (30 kHz) which always produce source wave with 6 points length [14], [20]. However, for CC_{excel} (cross-correlation by using excel), equation 4 was used to get the highest value of the normalized correlation coefficient; consequently, the corresponding time for this value

was taken at the time from normalized cross-correlation from excel.

$$CC\text{-norm}_{\text{excel}} = \frac{\sum_{T=0}^{T-1} X(T)Y(T)}{\sqrt{\sum_{T=0}^{T-1} X^2(T)} \sqrt{\sum_{T=0}^{T-1} Y^2(T)}} \quad (4)$$

In which $CC\text{-norm}_{\text{excel}}$ is the normalized correlation coefficient. T is corresponds to the signal time record, $Y(T)$ corresponds to source signal and $X(T)$ is corresponds to receiver signal.

Fifth method, was cross-correlation, which was calculated from the GDS software CC_{GDS} . Equation 5 was used to determine CC_{GDS} from GDS bender element analysis tools BEAT [21].

$$CC_{xy}(t_s) = \frac{1}{T} \sum_{T=0}^{T-1} X(T)Y(T+t_s) \quad (5)$$

In which $CC_{xy}(t_s)$ is the time for maximum value of cross-correlation, t_s is the time shift for source signal, T is corresponds to the signal time record, $Y(T)$ is corresponds to source signal and $X(T)$ is corresponds to receiver signal.

However, the damping-slope was calculated by calculating the damping ratio according to the differential between the amplitude of maximum source to the maximum receiver. This ratio was taken from the data only thus; the normalized data were ignored in damping calculations. However, even the measurement unit of the source signal was in volt (v) and the unit of the receiver was in millivolt (mv), the measuring unit was ignored to simplest the damping ratio.

3.0 RESULTS

3.1 Velocities Results

Figures 4, 5, 6 and 7 show the results for the P-wave and S-wave velocities for different horizontal distances D_r and ratio of horizontal distances to sample thickness $D_r:D$ at the sample thickness was 63.17 mm. In other side, in this research the ratio of horizontal distance to vertical distance will be expressed as percentage % and as $D_r:D$ where D_r is the horizontal distance and D the vertical distance (figure 3). However, the wave velocities were calculated via five different methods, visually, first-peak, maximum-peak, cross-correlation from excel (CC_{excel}) and cross-correlation from GDS software (CC_{GDS}). Figures 4 and 5 show that the P-wave and S-wave velocities can be detected (relative ease) until the horizontal distance reach 30 mm (when the ratio of horizontal distance to vertical distance $D_r:D$ equal 0.5:1) then it became difficult to detect the velocities from most of the methods. In other side, for P-wave velocities, the visual and first-peak showed similarity in the results within a horizontal distance range equal from 0 to 30 mm (when the ratio of horizontal distance to vertical distance from 0:1 to 0.5:1). Thus, the visual record could not be recognized after 30 mm horizontal

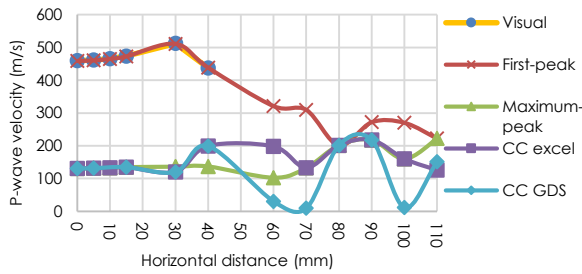


Figure 4 Plot of the horizontal distance D versus the P-wave velocities calculated from different methods (visual, first-peak, maximum-peak, CC_{excel} and CC_{GDS})

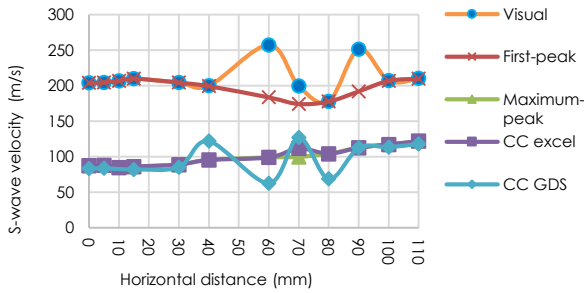


Figure 5 Plot of the horizontal distance D versus the S-wave velocities calculated from different methods (visual, first-peak, maximum-peak, CC_{excel} and CC_{GDS})

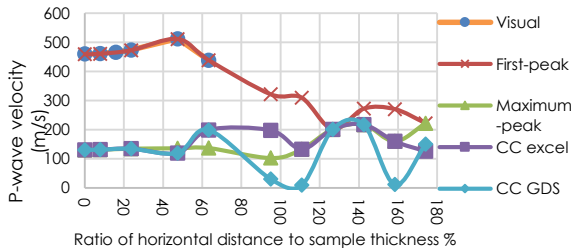


Figure 6 Plot of the ratio of horizontal distance to thickness Dr:D versus the P-wave velocities calculated from different methods (visual, first-peak, maximum-peak, CC_{excel} and CC_{GDS})

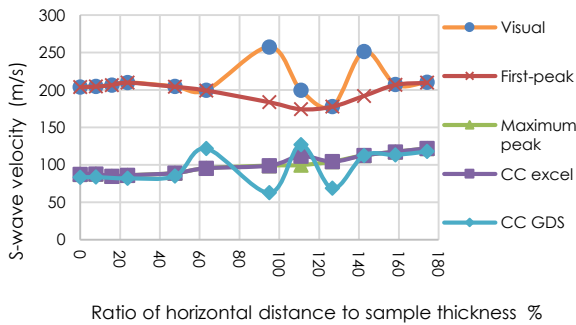


Figure 7 Plot of the ratio of horizontal distance to thickness Dr:D versus the S-wave velocities calculated from different methods (visual, first-peak, maximum-peak, CC_{excel} and CC_{GDS})

distance. However, the visual record appears continuously to the end for S-wave velocities.

Table 1 shows the results of wave velocities. The results within rang 0 to 30 mm horizontal distance (when Dr:D from 0:1 to 0.5:1), shows that the P-wave velocities, which were calculated from visual and first-peak being higher velocities (within range from 459 to 512 m/s) compare with other three methods. In other side, the velocities that were calculated from the maximum-peak, cross-correlation from excel (CC_{excel}) and cross-correlation from GDS software (CC_{GDS}) methods were within range from 120 to 136 m/s. The same pattern was for the S-wave velocities, which were between 203 to 209 m/s for visual and first-peak compare with 83 to 88 m/s for from maximum-peak, CC_{excel} and CC_{GDS} methods. In the other hand, table 1 shows also that the P-wave velocities were more varied than the S-wave velocities in the range when Dr: D above 0.5:1. The P-wave velocities in the range 0.5:1 were as the following: For visual was not detected. For first-peak, P-wave velocities within range from 158 to 438 m/s. For other methods within range 12 to 217 m/s.

The same for S-wave velocities was as the following: For visual and first-peak within the range 174 to 257 m/s. For other methods within range 50 to 124 m/s (figures 4; 5; 6; and 7).

Figure 8 shows an example of the way to detect the arrival time in the first-peak and maximum-peak. Where a figure 8a during use the direct data from the GDS software, and figure 8b with using the normalize data. The normalized source data were corresponding to the maximum positive value of source data and the same was for the normalized receiver data.

Table 1 Results of wave velocities obtained from the five analysed methods

Dr:D	Wave type	Visual	First-peak	Maximum-peak	CC _{excel}	CC _{GDS}
		m/s	m/s	m/s	m/s	m/s
0:1 to 0.5:1	P	459 to 512	458 to 510	131 to 136	120 to 134	120 to 134
above 0.5:1	P	Not detected	158 to 438	76 to 217	76 to 217	12 to 201
0:1 to 0.5:1	S	203 to 209	203 to 209	84 to 88	84 to 88	83 to 85
above 0.5:1	S	177 to 257	174 to 215	95 to 121	95 to 124	50 to 121

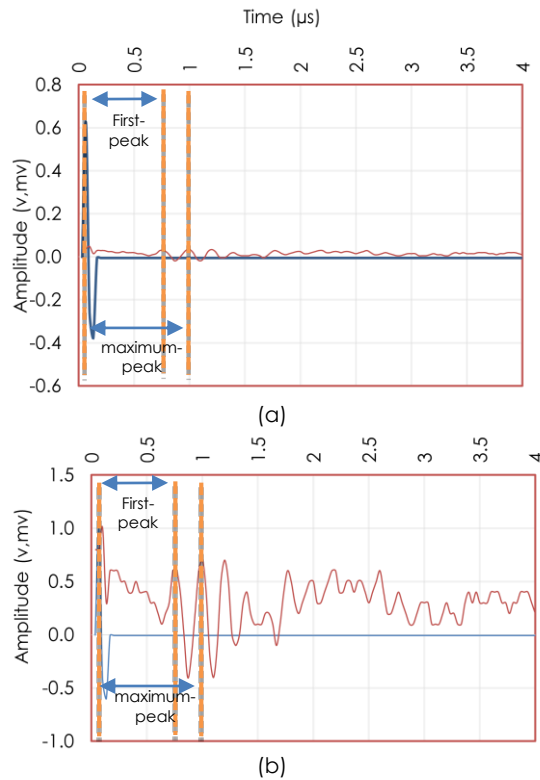


Figure 8 Shear wave sine signal with 30 kHz frequency for sample thickness 91.51 mm and horizontal distance equal to 30 mm. (a) Source and receiver data; (b) Normalized source and normalized receiver

3.2 Damping-Slope Results

Figures 9 and 10 show the results of damping versus a ratio of horizontal distance to sample thickness $Dr:D$ for sample with thickness equal to 63.17 mm. The results show that the damping-slope in P-wave and S-wave has similarity with increasing the Dr from zero point (i.e. $Dr:D = 0:1$) to the Dr equal to 110 mm (i.e. $Dr:D$ equal to 1.75:1). The damping for P-wave was within range from 5.6 to 31.7 % and the one for S-wave was within range from 1.9 to 31.3% (see table 2).

However, at the sample with thickness equal to 91.51 mm, both of the P-wave and S-wave can be classified to two zones (ranges) according to the slope of the damping-slope as it is shown in figures 11 and 12 and table 2. The first zone, when $Dr:D$ is less than 0.5:1 (i.e. 50% of ratio of Dr to D). The second zone, when $Dr:D$ is above than 0.5:1 (i.e. above 50% of ratio of Dr to D). At first zone ($Dr:D < 0.5:1$), the damping ratio is within range from 2.7 to 4.6 % for P-wave and from 2.9 to 3.9 % for S-wave. Also for second zone ($Dr:D$ above 0.5:1), the damping ratio is within range from 5.7 to 22.4 % for P-wave and from 5.5 to 20.5 % for S-wave.

According to table 2 and figures 13 and 14, the first zone (when $Dr:D < 0.5:1$, i.e. the ratio Dr to $D < 50\%$), the damping-slope as the following: For P-wave, the slope was equal to 0.7° with R^2 equal to 0.731. For S-

wave, the slope was equal to 0.9° with R^2 equal to 0.914. Moreover, the second zone (when $Dr:D > 0.5:1$, i.e. the ratio Dr to $D > 50\%$), the damping-slope as the following: For P-wave, the slope was equal to 13.7° with R^2 equal to 0.847. For S-wave, the slope was equal to 15.2° with R^2 equal to 0.936.

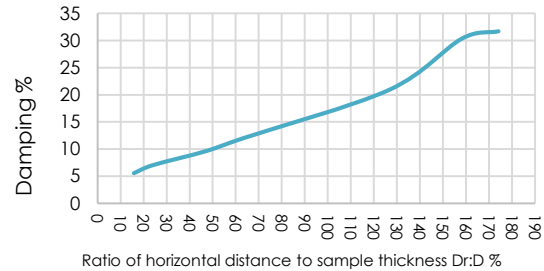


Figure 9 The Plot of the ratio of horizontal distance to thickness $Dr:D$ versus the P-wave damping for sample thickness 63.17 mm

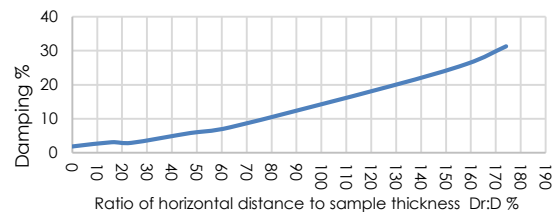


Figure 10 The Plot of the ratio of horizontal distance to thickness $Dr:D$ versus the S-wave damping for sample thickness 63.17 mm

Table 2 Results of Damping-slope for P-wave and S-wave

D	Wave type	Dr	$Dr:D$	Ratio of Dr to D	Damping ratio range	Damping-slope range
mm		mm	X:X	%	%	degree
63.17	P	0 to 110	0:1 to 1.75:1	0 to 100	5.6 to 31.7	-
63.17	S	0 to 110	0:1 to 1.75:1	0 to 100	1.9 to 31.3	-
91.51	P	0 to 45	0:1 to 0.5:1	0 to 50	2.7 to 4.6	0.0196
91.51	P	> 45	> 0.5:1	> 50	5.7 to 22.4	0.2784
91.51	S	0 to 45	0:1 to 0.5:1	0 to 50	2.9 to 3.9	0.0181
91.51	S	> 45	> 0.5:1	> 50	5.5 to 20.5	0.152

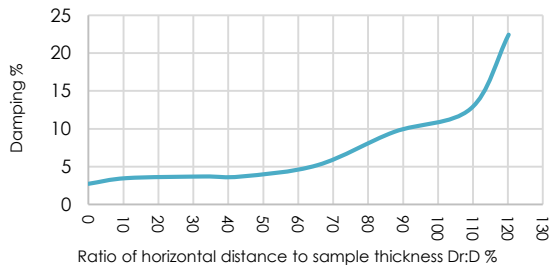


Figure 11 The Plot of the ratio of horizontal distance to thickness Dr:D versus the P-wave damping for sample thickness 91.51 mm

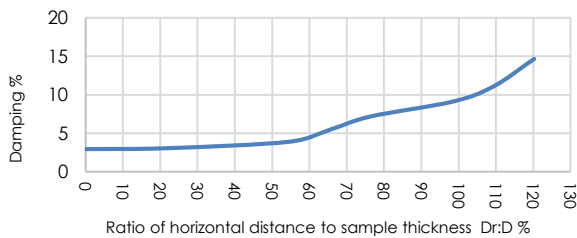


Figure 12 The Plot of the ratio of horizontal distance to thickness Dr:D versus the S-wave damping for sample thickness 91.51 mm

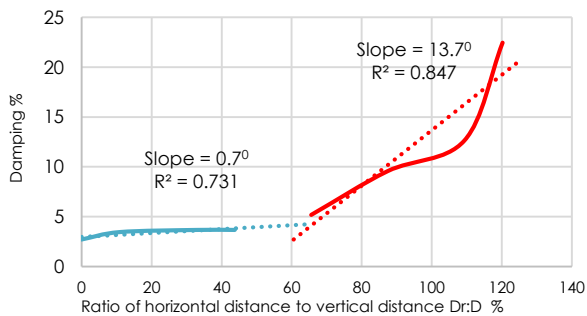


Figure 13 Slope of P-wave damping-slope in the range 0 to 50% (i.e. Dr:D below 0.5:1) (blue line) and range 50 to 120 % (i.e. Dr:D above 0.5:1) (red line) for sample thickness 91.51 mm

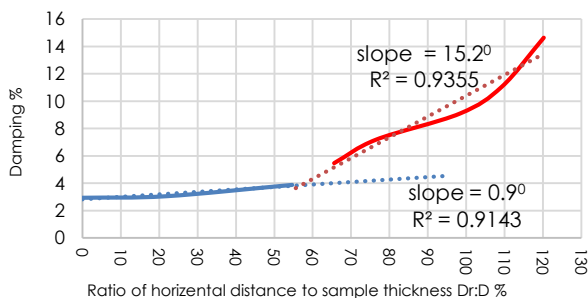


Figure 14 Slope of S-wave damping-slope in the range of 0 to 50% (i.e. Dr:D below 0.5:1) (blue line) and range 50 to 120 % (i.e. Dr:D above 0.5:1) (red line) for sample thickness 91.51 mm

4.0 DISCUSSION

By referring to Figures 6 and 7, it seems that both P-wave and S-wave velocities show uncertain in the calculated velocities with all methods when the alignment of the transmitter and receiver above 27° degree, where the ratio of horizontal distance to the thickness Dr:D equal to 0.5:1 (see Figure 3). These results should give caution to use the bender element in an alignment position such as the one, which used in the horizontal receiver sensor in the triaxial cell [10]. However, the results show that the visual reading (which were taken directly from the screen of the software on the bender element) can be difficult to recognize (or to provide certain value) when the damping increase rapidly. In other side, even the first-peak has the same rule as the visual one for determining the arrival time, but it can be easier to recognize than the visual one, especially when the data subjected to normalize.

The data that calculated from the maximum-peak and both cross-correlation from excel (CC_{excel}) and cross-correlation from GDS software (CC_{GDS}) always give similarity in the calculation of the arrival time. In addition, these methods exhibited arrival time longer than the one that was calculated by visually and first-peak. These results similar to what previous researcher found [1], [8], [14], [18], [19], [22].

In other side, for damping-slope (especially for S-wave), the results show a slight increase in the damping at the first zone when Dr:D within range from 0:1 to 0.5:1. Thus, this damping-slope start to increase rigidity at the second zone (within range of Dr:D above 0.5:1).

5.0 CONCLUSION

The conclusion drawn from this study are as follows:

1. Both of visual and first-peak have similarity in the results. Both of them provide velocities higher than the other three methods. Moreover, there are similarities between the maximum-peak, and CC_{excel} (cross-correlation from excel) and CC_{GDS} (cross-correlation from BEAT GDS software) methods provide.
2. The calculation of arrival time, become uncertain when the ratio of horizontal distance to the thickness of the sample Dr:D above 0.5:1 (i.e. ratio of Dr to D above 50 %) when the angle between transmitter to receiver above 27° .
3. For sample with thickness equal to 91.51 mm, the damping-slope for both P-wave and S-wave show differently, where can be divided into two zones (ranges of the ratio between the horizontal distance to thickness Dr:D). At first zone (when Dr:D from 0:1 to 0.5:1), the damping show a slight slope while this slope becomes steeply when the ratio of Dr:D cross above 0.5:1. This condition did not appear in the sample with thickness 63.17 mm.

Acknowledgement

The authors would like to thank the Ministry of Higher Education of Malaysia and RECESS of University Tun Hussein Onn Malaysia in providing the research grant Vot. U260 to undertaking this research.

References

- [1] Leong, E. C., Cahyadi, J. and Rahardjo, H., 2009. Measuring Shear and Compression Wave Velocities of Soil Using Bender-Extender Elements. *Can. Geotech. J.* 46: 792-812.
- [2] Rio, J. F. M. E. 2006. *Advances in Laboratory Geophysics Using Bender Elements*. Doctoral dissertation, University of London.
- [3] Jong-Sub Lee and J. Carlos Santamarina. 2005. Bender Elements: Performance and Signal Interpretation. *Journal of Geotechnical and Geoenvironmental Engineering*. 131(9). September 1, 2005. ©ASCE, ISSN 1090 0241/2005/9-1063-1070.
- [4] Christophe, D. Hocine, H. and Pierre-Yves, H. 2003. Characterization of Loire River Sand in the Small Strain Domain Using New Bender-Extender Elements. *16th ASCE Engineering Mechanics Conference*, July 16-18, 2003, University of Washington, Seattle, USA.
- [5] Arulnathan, R., Boulanger, R. W., Kutter, B. L., and Sluis, W. K. 2000. New Tool for Shear Wave Velocity Measurements in Model Tests. *ASTM Geotechnical Testing Journal*. 23(4): 444-453.
- [6] Jovicic, V., Coop, M. R. and Simic, M. 1996. Objective Criteria for Determining Gmax from Bender Element Tests, Technical Note. *Geotechnique*. 46(2): 357-362.
- [7] Brignoli, E. G. M., Gotti, M., and Stokoe, K. H. 1996. Measurement of Shear Waves in Laboratory Specimens By Means Of Piezoelectric Transducers. *ASTM Geotechnical Testing Journal*. 19(4): 384-397.
- [8] Viggiani, G. and Atkinson, J. H. 1995a. Interpretation of Bender Element Tests, Technical Note. *Geotechnique* 45(1): 149-154.
- [9] Viggiani G. and Atkinson, J. H. 1995b. Stiffness of Fine-Grained Soil at Very Small Strains. *Geotechnique*. 45(2): 249-265.
- [10] Clayton, C. R. I., Theron, M., and Best, A. I. 2004. The Measurement of Vertical Shear-Wave Velocity using Side-Mounted Bender Elements in the Triaxial Apparatus. *Geotechnique*. 54(7): 495-498.
- [11] Germano, C., 2003. Flexure Mode Piezoelectric Transducers. Audio and Electroacoustics. *IEEE Transactions*. 19(1):6.
- [12] Lawrence, F. V., 1965. *Ultrasonic Shear Wave Velocity in Sand and Clay*. Massachusetts Institute of Technology, Cambridge, Mass. Research Report R65-05.
- [13] Lings, M. L. and Greening, P. D. 2001. A Novel Bender/Extender Element for Soil Testing, Technical Note. *Geotechnique* 51(8): 713-717.
- [14] Leong, E. C., Yeo, S.H., and Rahardjo, H. 2005. Measuring Shear Wave Velocity Using Bender Elements. *Geotechnical Testing Journal*. 28(5): 488-498.
- [15] Alramahi, B. 2007. *Characterization Of Unsaturated Soils Using Elastic And Electromagnetic Waves*. Doctoral Dissertation, Department of Civil and Environmental Engineering, Louisiana State University.
- [16] Sa'nchez-Salinero, I., Roesset, J. M. and Stokoe, K.H. 1986. *Analytical Studies of Body Wave Propagation and Attenuation*, Geotechnical Engineering Report No GR86-15. Civil Engineering Department, University of Texas at Austin. 272 pages.
- [17] Knox, D. P.; Stokoe, K. H. and Kopperman, S. E., 1982. *Effect of State of Stress on Velocity of Low Amplitude Shear Wave Propagating Along Principal Stress Directions in Dry Sand*. Geotechnical Engineering Research Report GR 82-23. University of Texas at Austin.
- [18] Yamashita, S., Kawaguchi, T., Nakata, Y., MIKAML, T., Fujiwara, T., and Shibuya, S. 2009. Interpretation of International Parallel Test on the Measurement of Gmax Using Bender Elements. *Soils and foundations*. 49(4): 631-650.
- [19] Arulnathan, R., Boulanger, R.W., and Riemer, M.F., 1998. Analysis of Bender Element Tests," *Geotechnical Testing Journal*. 21(2): 120-13.
- [20] Zarar, M.M.J. Personal Communication. Center of Electromagnetic Compatibility EMC, Universiti Tun Hussein Onn Malaysia UTHM. Johor, Malaysia. April 10, 2014.
- [21] Rees, S., Le Compte, A., and Snelling, K. 2013. A New Tool for the Automated Travel Time Analyses of Bender Element Tests. *Proceedings of the 18th International Conference on Soil Mechanics and Geotechnical Engineering*, Paris 2013.
- [22] Yang, J., and Gu, X. Q. 2013. Shear Stiffness of Granular Material at Small Strains: Does It Depend on Grain Size?. *Geotechnique*, 63(2): 165-179.